Global Flow Measurement Workshop
25 - 27 October 2022

Technical Paper

Accurate Coriolis Mass Flow and Density Measurement of Bubbly Fluids

Daniel L. Gysling, CorVera, LLC

ABSTRACT

This paper presents experimental data quantifying errors in the mass flow and density from two modern, dual bent-tube Coriolis meter operating on bubbly mixtures of air and water with gas void fractions ranging from 0% to ~5%. Additionally, theoretical development and experiment validation of speed of sound augmented Coriolis meters, developed to improve the accuracy of Coriolis meters operating on bubbly flows, are presented. By improving the ability of Coriolis meters to measure bubbly flows, speed of sound augmented Coriolis meters offer the potential to broadly expand the application space of Coriolis meters to address many potentially multiphase measurement challenges.

The sources of measurement errors in Coriolis meters operating on bubbly liquids have been well-characterized in the literature. In general, conventional Coriolis meters interpret the mass flow and density of the process fluid using calibrations developed for single-phase process fluids that are essentially incompressible and essentially homogeneous. While these calibrations typically provide sufficient accuracy for single-phase flow applications, their use on bubbly flows often results in significant errors in both the reported mass flow and density. Speed of sound augmented Coriolis meters utilize a process fluid sound speed measurement and an empirically-informed aeroelastic model of bubbly flows in Coriolis meters to compensate output of conventional Coriolis meters for the effects of entrained gas to provide accurate mass flow, density, volumetric flow, and gas void fraction of bubbly liquids.

Data presented are limited to air and water mixtures. However, by influencing the effective bubble size through mixture flow velocity, the bubbly mixtures tested exhibit a wide range of decoupling characteristics, spanning theoretical limits from nearly fully-coupled to nearly fully-decoupled flows. Thus, from a non-dimensional parameter perspective, the data presented is representative a broad range of bubbly flows likely to be encountered in practice.

1 INTRODUCTION

Coriolis flow meters offer high-accuracy, low maintenance and calibration requirements, high-turndown ratios, and multi-variable measurement capabilities. For these and other reasons, Coriolis meters are the flow meter of choice for many applications [1]. Coriolis meters typically excel at single-phase liquid applications; however, the accuracy of Coriolis meters is well-known to degrade in bubbly flow conditions [2]. This decreased accuracy in bubbly flows serves to limit both the adoption rate and the utility of Coriolis meters in many applications where bubbly flow conditions are either consistently, or intermittently, present.

Over the past ~20 years, Coriolis manufacturers have significantly improved the operability of Coriolis meters in bubbly flows with digital controllers [3]. Unlike earlier-generation Coriolis meters with analog controllers, modern digital Coriolis meters can typically continue to operate in the presence of significant amounts of entrained gases, providing mass flow and density measurements based on single-phase interpretations of their fundamental measurements. Unfortunately, mass flow and density measurements reported by Coriolis meters operating on bubbly flows utilizing calibrations developed for single-phase flows often contain significant measurement errors.

To address this well-known reduction in accuracy for Coriolis meters operating on bubbly flows, Coriolis manufacturers have developed best-practices and software processing algorithms to mitigate measurement errors associated with bubbly fluids [2]. These best-practices advise end-users to minimize entrained gas void fraction, increase mixture velocities, and orient Coriolis meters in specific ways with respect to gravity. While these best practices are often helpful in reducing errors due to bubbly flow, implementing these best practices may not be practical in many applications, or may result insignificant compromises the process. Therefore, despite progress in both maintaining operability and providing error mitigation strategies for bubbly flow conditions, there remains a need for solutions that enable Coriolis meters to maintain near single-phase accuracy on generalized bubbly flows by fundamentally addressing, and compensating for, errors developed in Coriolis meters operating bubbly flows.

This paper presents a theoretical development and experimental validation of an approach to utilize a process fluid speed-of-sound measurement to augment Coriolis meters operating in bubbly flows. The approach utilizes a process fluid speed of sound measurement to quantify gas void fraction and the reduced frequency of the Coriolis flow tube vibration. This information is then used within an empirically-informed, first-principles aeroelastic model of the effects of bubbly flows in Coriolis meters to improve the accuracy of Coriolis meters operating on bubbly flows.

By improving the accuracy of Coriolis meters operating on bubbly flows, speed-of-sound augmented Coriolis meters offer the potential for Coriolis meter to more-effectively address many applications in which bubbly flow may, or may not, be present. Within the energy industry, these applications include net-oil measurement from separator outlet flows with gas carry-under, drilling fluid return lines, and Lease Automatic Custody Transfer (LACT) measurements, as well as challenges associated with the low-carbon energy transition such as measuring carbon dioxide (CO_2) and liquefied natural gas (LNG) which are often processed at conditions near, or at, phase transition boundaries.

2 CORIOLIS FLOW METER ERRORS DUE TO BUBBLY LIQUIDS

The sources of measurement errors in Coriolis meters operating on bubbly liquids have been well-documented in the literature [4],[5],[6],[7],[8]. Coriolis meters determine the mass flow and density of a process fluid by measuring and interpreting the effect that the process fluid has on the vibrational characteristics of one or more vibrating flow tubes. For bent tube Coriolis meters, Coriolis forces on the fluids flowing through the flow tubes results in a deformation, or twist, in the fundamental vibration mode of the fluid conveying flow tubes. This deformation of the vibration mode is measured determining the phase lag between signals generated by pick-off coils measuring the relative velocity of the opposing outbound and inbound flow tubes[1]. For single phase fluids, the twist developed between the outwardly flowing section of a flow tube and the inwardly flowing section of a flow tube is proportional to the mass flow rate of the process fluid. Similarly for density, the mass of the process fluid loads the vibration mode of the fluid-conveying flow tubes, resulting in the natural frequency of the vibrational mode of the process fluid-conveying flow tubes scaling inversely with the density of the process fluid[1].

In general, conventional Coriolis meters determine the mass flow and density of the process fluid using calibrations developed for single-phase fluids, i.e. fluids that are both essentially incompressible and essentially homogeneous. While these calibrations are typically sufficiently accurate for a wide range of single-phase flow applications, their use on bubbly flows often results in significant errors in both the reported mass flow and the reported density. As developed in the literature, these errors can be attributed to decoupling effects associated with the inhomogeneity of bubbly flows, and compressibility effects associated with the increased compressibility of bubbly flows compared to single phase flows.

Several authors have presented models describing the effect of bubbly fluids on Coriolis meters. Hemp, 2006, [5] presented a model for the errors developed in Coriolis meters operating on bubbly flows that provides a concise formulation for the errors associated with both decoupling and compressibility.

Hemp's model predicts that the density measured by a Coriolis meter, calibrated on an essentially homogeneous and incompressible single-phase flow, but operating on a bubbly flow, is related to the density of the liquid phase as follows:

$$\boldsymbol{\rho_{meas} = \rho_{liq}\left(1 - K_d\alpha + G_d f_{red}^2\right)} \quad (1)$$

Where ρ_{meas} is the measured density, ρ_{liq} is the density of the liquid phase, α is gas void fraction, f_{red} is the reduced frequency, defined below:

$$f_{red} \equiv \frac{2\pi f_{tube} D/2}{a_{mix}} \qquad (2)$$

Where $\boldsymbol{f_{tube}}$ is the vibrational frequency of the tube, D is the inner diameter of the tube, and $\boldsymbol{a_{mix}}$ is the sound speed of the process fluid. The reduced frequency is a non-dimensional number that characterizes the impact of a fluid compressibility Coriolis flow meters [4]. K_d is the density decoupling parameter and K_d quantifies the effect of decoupling on the density measured by a Coriolis meter operating on of a bubbly flow.

The density decoupling parameter is theoretically linked to the decoupling ratio, defined as the ratio of vibrational amplitude of gas bubbles compared to that of the liquid phase in the transverse oscillations of the fluid-conveying flow tubes. Figure 1, adapted from (Weinstein, 2006) [7] shows an approximation of the decoupling ratio of a bubbly mixture as a function of inverse Stokes number. The inverse Stokes number is defined as follows:

$$\delta \equiv \sqrt{\frac{2\mu}{\rho_{liq} 2\pi f_{tube} R_{bubble}^2}} \qquad (3)$$

Where μ is the dynamic viscosity of the liquid phase, ρ_{liq} is the density of the liquid, and R_{bubble} is the representative radius of the bubbles. The smaller the inverse Stokes number, (i.e., less viscous fluids, larger sized bubbles, higher vibrational frequency), the more decoupling that occurs. Theoretically, the maximum decoupling occurs at the inviscid limit, associated with the inverse Stokes number approaching zero. As shown in Figure 1, in the limit of inverse Stokes number approaching zero, the decoupling ratio approaches three (K_d➔3). For large inverse Strokes numbers, the bubbles become 'fully-coupled' to the liquid phase and the effects of decoupling are eliminated and K_d approaches unity (K_d➔1).

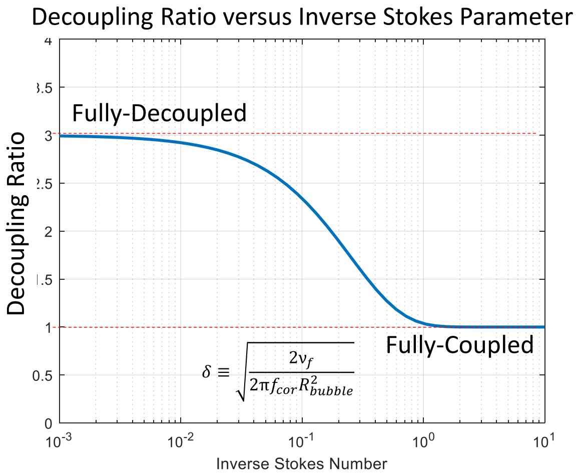

Figure 1: Decoupling Ratio of a Gas Bubble with a Liquid as a function of Inverse Stokes Number

In Hemp's formulation [5], the effect of compressibility is captured by the product of G_d, the density compressibility parameter, and the square of the reduced frequency, $\boldsymbol{f_{red}^2}$. Hemp suggests a value of G_d=0.25 for the density compressibility parameter. For positive values of K_d and G_d, the effects of decoupling and compressibility generate offsetting errors in the measured density of bubbly flows, with decoupling effects causing under-reporting of liquid density and compressibility effects causing an over-reporting of liquid density.

Similarly for mass flow, Hemp's model predicts that the mass flow measured by a Coriolis meter operating on a bubbly liquid is related to the mass flow of the liquid as follows:

$$\dot{m}_{meas} = \dot{m}_{liq}\left(1 - \frac{(K_m - 1)}{1-\alpha}\alpha + G_m f_{red}^2\right) \quad (4)$$

Where K_m is the mass flow decoupling parameter (1>K_m>3) and G_m is the mass flow compressibility parameter. Hemp suggests a value for the mass flow compressibility parameter of G_m =0.5.

3 SPEED OF SOUND AUGMENTED CORIOLIS FLOW METERS

The use of speed of sound measurements to improve the interpretation of Coriolis flow meters operating on bubbly flows was first developed using clamp-on SONAR-based gas void fraction meters to improve density-based watercut measurements of Coriolis meters operating on bubbly flows on the liquid outlet of two-phase separators [9]. This early application of speed of sound augmented Coriolis meters assumed that the bubbly liquid within the Coriolis meter was fully-coupled (K_d➔1) and essentially incompressible ($f_{red}^2 \ll 1$). The work presented in this paper further extends this and other work to provide a means to improve both the mass flow and density of Coriolis meters operating bubbly flows exhibiting a wider range of decoupling and compressibility effects.

Speed of sound augmented Coriolis meters utilize a process fluid sound speed measurement integrated with the output of a conventional Coriolis meter to compensate errors in the reported mass flow and density associated with decoupling and compressibility effects exhibited by bubbly flows. As developed theoretically by Gysling et al [10], the addition of a process fluid sound speed measurement to the mass flow and density measurements of a Coriolis meters provides additional information to improve the accuracy and utility of Coriolis meters operating on bubbly fluids.

The speed of sound of bubbly fluids is fundamentally linked to the both the gas void fraction and the reduced frequency of a Coriolis meter, each of which are important parameters associated with the effect of decoupling and compressibility, respectively. This enables speed of sound augmented Coriolis meters to provide mass flow, density, and volumetric flow measurement of bubbly liquids with near single-phase accuracy, while also providing accurate quantification of gas void fraction of bubbly liquids.

For sound propagating within a conduit for which the wavelength is large compared to both fluid inhomogeneities and the cross-sectional length scale of the conduit, Wood's equation [11] relates mixture sound speed, a_{mix}, and density, ρ_{mix} of a mixture consisting of "N" components to the phase fractions, φ_i , density, ρ_i and sound speeds, a_i of each of the i^th components of the mixture. The elasticity of the conduit, E, also enters into Wood's Equation, given below for a thin-walled, circular cross section conduit of outer diameter D and wall thickness of t.

$$\frac{1}{\rho_{mix} a_{mix}^2} = \sum_{i=1}^{N} \frac{\varphi_i}{\rho_i a_i^2} + \frac{D-t}{Et} \qquad (5)$$

Where mixture density, ρ_{mix}, is given by:

$$\rho_{mix} = \sum_{i=1}^{N} \rho_i \, \varphi_i \qquad (6)$$

For bubbly liquids, Wood's equation can be expressed as follows:

$$\frac{1}{\rho_{mix} a_{mix}^2} = \frac{\alpha}{\rho_{gas} a_{gas}^2} + \frac{1-\alpha}{\rho_{liq} a_{liq}^2} + \frac{D-t}{Et} \qquad (7)$$

Where the mixture density is given by:

$$\rho_{mix} = \alpha \rho_{gas} + (1-\alpha)\rho_{liq} \qquad (8)$$

The measured speed of sound can be expressed as a function of the gas void fraction and the fluid properties and properties of the conduit as follows:

$$a_{mix} = sqrt\left(\frac{1}{\left(\rho_{mix}\left(\frac{\alpha}{\rho_{gas} a_{gas}^2} + \frac{1-\alpha}{\rho_{liq} a_{liq}^2} + \frac{D-t}{Et}\right)\right)}\right) \qquad (9)$$

For cases in which the compressibility of the gas phase is dominant, which is typically a good approximation for gas void fraction on the order of 0.1% or greater, the gas void fraction scales with the inverse of the square of the process fluid sound speed:

$$\alpha \cong \frac{\gamma P}{\rho_{liq} \boldsymbol{a_{mix}^2}} \qquad (10)$$

Where γ is the ratio of specific heats of the gas and P is the process pressure. Using this approximation for the gas void fraction, Hemp's model for the relationship between the density measured by a Coriolis meter operating on bubbly flows and liquid density with constant process and Coriolis parameters, and the liquid density can be expressed as a linear function of gas void fraction:

$$\rho_{meas} = \rho_{liq}(1 - K_d\alpha + G_d f_{red}^2) \cong \rho_{liq}\left(1 - \left\{K_d - G_d \frac{\rho_{liq}}{\gamma P}(2\pi f_{tube} D/2)^2\right\}\alpha\right) \quad (11)$$

For a given Coriolis meter operating on bubbly liquids at a given process condition, the influence of compressibility scales with a non-dimensional compressibility influence parameter, Γ, defined as:

$$\Gamma \equiv \frac{\rho_{liq}}{\gamma P}(2\pi f_{tube} D/2)^2 \quad (12)$$

Using the definition of the compressibility influence parameter, Γ, the measured density can be expressed as:

$$\rho_{meas} \cong \rho_{liq}(1 - \{K_d - G_d\Gamma\}\alpha) \quad (13)$$

The above expression can be used to define a compressibility-adjusted density decoupling parameter, $K_{d_{eff}}$, as follows:

$$\rho_{meas} \cong \rho_{liq}\left(1 - K_{d_{eff}}\alpha\right) \quad (14)$$

Where the compressibility-adjusted density decoupling parameter, $K_{d_{eff}}$, theoretically represents the slope of the measured mixture density versus gas void fraction for a bubbly mixture with constant mixture properties but varying gas void fraction and is defined as:

$$K_{d_{eff}} \equiv K_d - G_d\Gamma \quad (15)$$

Similarly for mass flow, assuming constant process parameters and small gas void fraction ($\alpha << 1$), the measured mass flow can also be expressed as a linear function of gas void fraction as follows:

$$\dot{m}_{meas} = \dot{m}_{liq}\left(1 - \frac{(K_m - 1)}{1-\alpha}\alpha + G_d f_{red}^2\right) \cong \dot{m}_{liq}(1 - \{K_m - 1 - G_m\Gamma\}\alpha) \quad (16)$$

4 EXPERIMENTAL SETUP AND PROCEDURE

The current work investigates the effectiveness utilizing a process fluid sound speed measurement to augment the output of two, state-of-the-art, dual-bent-tube Coriolis meters to provide accurate measurement of the mass flow, liquid density, liquid volumetric flow, and gas void fraction of bubbly flows[1]. In this context, bubbly flows assumes that the entrained gas are well-mixed and well-distributed within a liquid-continuous phase.

The process fluid sound speed was measured utilizing passive-listening techniques to interpret the output of an array of pressure transducers installed on the process

[1] The manufacturers of each of the Coriolis meters evaluated in this paper offer software and/or hardware options designed to mitigate errors associated with bubbly liquids. Evaluation of these options was beyond the scope of this work.

piping external to, but spanning the length of, each Coriolis meter. Specifically, the first transducer was installed immediately upstream of the Coriolis meter under test, and a second and third pressure transducer were installed downstream of the Coriolis meter under test. No modifications were made to either of the Coriolis meters, or Coriolis meter transmitters, for these tests.

Parameters for the two, modern, state-of-the-art, Coriolis meters are listed Table 1. As indicated in Table 1, a primary difference between the two meters tested is the nominal vibrational frequency of Coriolis meter B having a vibration frequency of slightly more than twice that of Coriolis meter A.

Table 1: Parameters for Coriolis Meters Tested

	Number of Tubes	Nominal size (in)	Tube Shape	Nominal Vibrational Frequency with Water (Hz)	Assumed Flow tube ID (in)
Coriolis Meter A	2	2	U-shaped	80	1.06
Coriolis Meter B	2	2	U-shaped	175	1.1

The methodology used herein utilizes 1) a process fluid speed of sound measurement and 2) an empirically-informed, first-principles aeroelastic models of the effect of bubbly flow on errors developed in Coriolis meters operating on bubbly flows, calibrated on single-phase fluids. It is important to note that the measured data presented in this paper was collected with each Coriolis meter operating with its respective, optional bubbly flow mitigation capabilities disabled. Measured mass flow and density data from the Coriolis meter under test was then used as the basis for the speed of sound compensated mass flow and density measurements.

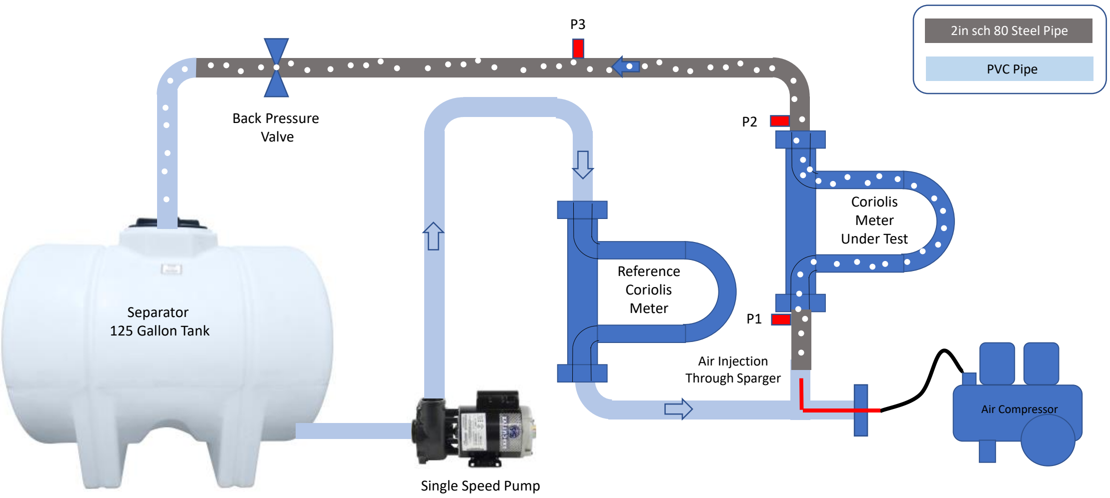

Figure 2: Schematic of Speed of Sound Augmented Coriolis Test Facility

Figure 2 shows a schematic of the flow loop facility used to measure, characterize and correct for, mass flow and density errors developed in Coriolis meters operating on bubbly mixture of air and water. The system consists of 1) a water tank that serves as a liquid reservoir and a gravity-based air/water separator; 2) single speed centrifugal water pumps; 3) a reference Coriolis meter operating on single-phase liquid from the outlet of the separator; 4) and air injection system; 5) a flag-mounted, vertically-upward flowing Coriolis meter under test; 6) an array of acoustic pressure transducers installed on the process piping which spans the Coriolis meter under test; 7) static pressure transducers measuring the pressure at the inlet and outlet of the Coriolis meter under test; and 8) an adjustable back pressure valve to control back pressure and flow rate. Note that the system utilized two, single-speed pumps, valved in a manner which allowed the pumps to be operated independently, in series, or in parallel to generate a wider range of pressure and flow conditions. The system was designed such that the reference Coriolis meter and the Coriolis meter under test were interchangeable, such that the Coriolis meter operating on the liquid outlet of the separator served as the reference meter for the Coriolis meter under test.

Data was acquired from the Coriolis meter under-test and the reference Coriolis meter for ninety second set points over which the nominal operating conditions of the flow loop, i.e., the pump speed, the back pressure valve, and air injection rates, were held constant for a series of gas injection rates. Concurrently, high frequency time-resolved pressure data was recorded from the array of acoustic pressure transducers installed on the process piping upstream and downstream of the Coriolis meter under-test. Additionally, data was recorded from static pressure measurements upstream and downstream of the Coriolis meter under-test.

Data was collected in a series of points in which the pump speed and back pressure valve position were fixed, and the amount of air injected was adjusted to create gas void fractions from 0% to >5%. The measured process fluid sound speed was used to determine the gas void fraction within the Coriolis meter under test for each data point. The amount of air injected was monitored using a variable area flow meter as reference during data collection; however, data from the variable area flow meter was not utilized in the data processing. The measured density and drive gain diagnostics of the reference Coriolis meter, operating on the outlet of the separator, were monitored to ensure that there was no significant gas carry-under from the liquid outlet of the separator tank. After each series of data points were recorded over a range of gas void fractions, the pump configuration and/or back pressure valve setting was adjusted to a different nominal flow rate and back pressure, and the process was repeated.

For each ninety second data point, the output of the array of pressure transducers was post-processed to determine the sound speed of the process fluid as function of time for each data set. Time-averaged values of the process fluid sound speed and measured density used iteratively to determine the gas void fraction for each data point and the liquid density for each set of data points for which the process conditions were held constant over a range of 0-5% gas void fraction.

5 MEASURED ERRORS DUE TO BUBBLY FLOW

The time-averaged mass flow, density and volumetric flow measured for each data point by each of the Coriolis meters operating in bubbly flow, normalized by the same values measured by the reference Coriolis operating on only the liquid phase of the bubbly mixture, are presented in Figure 3, Figure 4, and Figure 5, respectively.

5.1 Mass Flow Errors

Figure 3 shows the time-averaged measured mass flow, normalized by reference mass flow, versus gas void fraction for Coriolis meters A and B for a range of mixture velocities and pressures. As will be developed below, the nominal mixture velocities and pressure for each set are listed as dimensional quantities that qualitatively indicate the relative effects of decoupling and compressibility, respectively, for a given meter operating on bubbly mixtures of a given composition, e.g., in this case, air and water. Reference lines are also included in Figure 3 showing the theoretical values for the errors predicted using Hemp's model for fully-coupled and fully-decoupled conditions with negligible compressibility.

As shown in Figure 3, the mass flow data for Coriolis meter A operating in bubbly flow with nominally constant conditions with varying gas void fraction exhibits errors that scale essentially linearly with gas void fraction, with the mass flow error with gas void fraction increasing with decreasing mixture velocity. Additionally, the mass flow data from Coriolis meter A exhibits errors that essentially span the full range of the errors predicted by Hemp's model for flows that are fully-coupled (no error due to decoupling) to flows that are fully-decoupled (with errors equal to 2 times the gas void fraction). The errors in mass flow for Coriolis meter B are, in general, 1) smaller than those for Coriolis meter A, 2) exhibit a higher degree of non-linearity with gas void fraction, and 3) show a mixture of under-readings and over-readings.

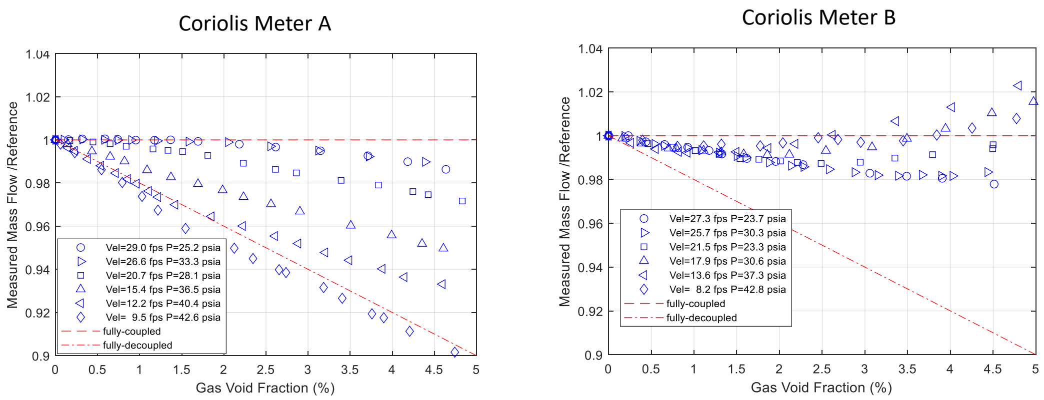

Figure 3 Measured Mass Flow normalized by reference Mass Flow versus Gas Void Fraction for Coriolis Meters A and B for a range of Mixture Velocities and Pressures

5.2 Density Errors

Figure 4 shows the time-averaged, measured density, normalized by reference liquid density, versus gas void fraction for Coriolis meters A and B for a range of mixture velocities and pressures. Reference lines are also included showing the theoretical values predicted by Hemp's model for a fully-coupled and a fully-decoupled conditions with negligible compressibility. As shown, the density data for Coriolis meter A and Coriolis meter B, each operating in bubbly flows with nominally constant conditions with varying gas void fraction, exhibit errors that scale essentially linearly with gas void fraction. Additionally, the density data from each meter exhibits characteristics that are consistent with a wide range of compressibility-adjusted density decoupling parameters.

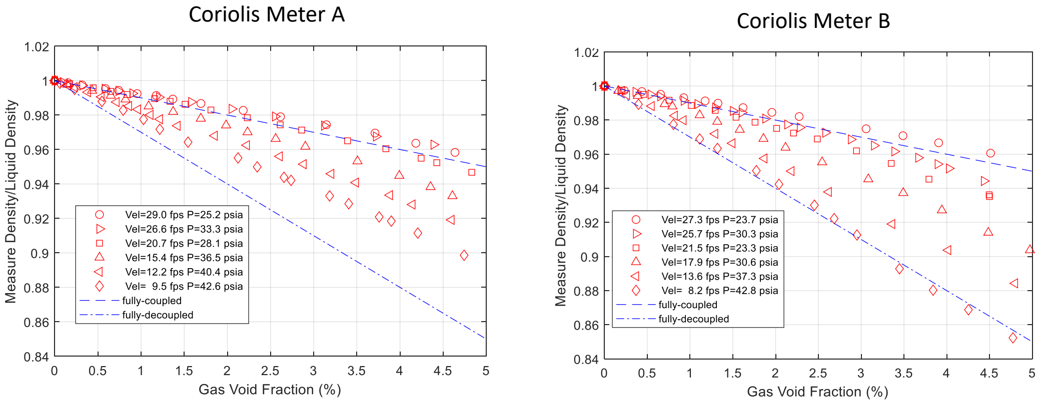

Figure 4 Measured Density normalized by reference Density versus Gas Void Fraction for Coriolis Meters A and B for a range of Mixture Velocities and Pressures

5.3 Volumetric Flow Errors

In addition to mass flow and density, Coriolis meters are often used to provide volumetric flow measurement. Unlike other types of flow meters, such as positive displacement flow meters and electromagnetic flow meters, Coriolis meters do not directly measure volumetric flow. rather, Coriolis meters calculate the volumetric flow by dividing the measured mass flow by the measured density. The volumetric flow reported by a Coriolis meter operating in bubbly flow can be expressed using Hemp's terminology as follows:

$$Q_{meas} = \frac{\dot{m}_{meas}}{\rho_{meas}} = \frac{\dot{m}_{liq}\left(1-\frac{(K_m-1)}{1-\alpha}\alpha+G_m f_{red}^2\right)}{\rho_{liq}\left(1-K_d\alpha+G_d f_{red}^2\right)} = Q_{liq}\,\frac{\left(1-\frac{(K_m-1)}{1-\alpha}\alpha+G_m f_{red}^2\right)}{\left(1-K_d\alpha+G_d f_{red}^2\right)} \qquad (17)$$

Thus, the errors in reported volumetric flow due to bubbly flows are a function of decoupling and compressibility errors in both the mass flow and density. Since gas void fractions are typically not known in most bubbly flow applications, and often assumed to negligible, the volumetric flow rate reported by a Coriolis meter operating on a bubbly liquid, is often interpreted as the volumetric flow rate of the liquid phase, similar to the density reported by a Coriolis meter operating on bubbly liquid often being interpreted as the density of the liquid phase.

Figure 5 shows the measured volumetric flow normalized by reference liquid volumetric flow versus gas void fraction for Coriolis meter A and Coriolis meter B for a range of mixture velocities and pressures. For reference, a (1+GVF) line corresponding to the theoretical error for a Coriolis meter exhibiting the same amount of decoupling for the mass flow and density (i.e. $K_d = K_m$) with negligible compressibility effects (i.e. $f_{red}^2 \rightarrow 0$) , is included in Figure 5. As shown, for Coriolis Meter A, the volumetric flow exhibits less percentage error than either the mass flow or the density for the majority of the data points. This reduced error in volumetric flow of bubbly liquids is due to the errors in the mass flow and density serving to offset each other to a varying degree. For Coriolis meter A, the largest errors in volumetric flow are reported for the conditions for which the decoupling was minimized, i.e., the highest mixture flow rates tested. For Coriolis meter B, however, the errors in liquid volumetric flow for the data points measured are significantly larger than the errors in mass flow. For Coriolis meter B the volumetric flow errors are driven primarily due to differences in the measured density and the density of the liquid phase. For Coriolis meter B, the largest errors in volumetric flow are over-readings associated with conditions exhibiting the largest compressibility-adjusted density decoupling parameters.

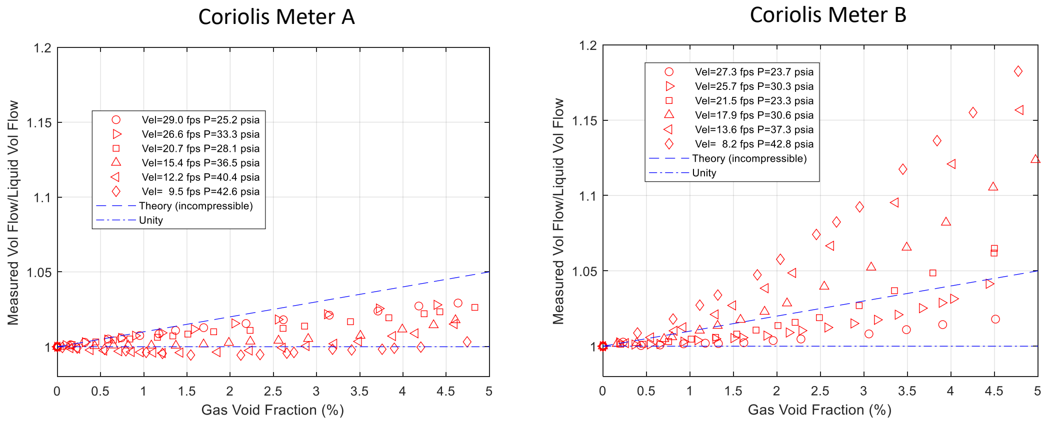

Figure 5: Measured Volumetric Flow normalized by reference Liquid Volumetric flow versus Gas Void Fraction for Coriolis Meter A and Coriolis Meter B for a range of Mixture Velocities and Pressures

6 DISCUSSION OF ERRORS DUE TO BUBBLY FLOW

For Coriolis meter A, the errors in both mass flow and density trend with the nominal mixture velocity within the flow tubes of the Coriolis meter under test, with data sets with slower mixture flow velocities exhibiting larger errors as a function of gas void fraction than the data sets with higher mixture flow velocities. This variation in the errors associated with bubbly flow scaling with flow velocity for the bubbly air/water mixtures can be attributed to the nominal bubble size scaling inversely with the mixture flow velocity as described in [2] for Coriolis meters. For bubble flows in general, the higher the flow rate, the greater the shear, and the smaller the average bubble size [12]. Since the other relevant gas and liquid properties are essentially constant for all the data sets presented, changing bubble size with mixture flow velocity changes the inverse Stokes number, δ. As shown, the data indicate that the conditions spanned a significant range of decoupling, ranging from nearly fully-coupled at the highest mixture velocities in the flow tubes tested, to nearly fully-decoupled at the lower range of mixture velocities tested.

This effect of mixture velocity on bubble size, and, in turn on decoupling characteristics, is reflected in the best practices advice from Coriolis manufacturers which recommends end-users increase flow velocities through Coriolis meters to minimize the errors due to bubbly flows in general, and decoupling specifically [2].

For Coriolis meter B, the mass flow errors are significantly less than the mass flow errors observed in Coriolis meter A. This relative insensitivity of the mass flow measurement to gas void fraction exhibited by Coriolis meter B for the conditions tested may be associated with over-reading effects due compressibility effectively balancing the under-reporting effects due to decoupling. Note that theoretical models by Hemp [5] and Zhu [8], predict that compressibility has 2x or greater effect on mass flow compared to density ($G_m \geq 2G_d$), qualitatively consistent with the data presented for Coriolis B.

7 MEASURED SOUND SPEED AND INTERPRETTED GAS VOID FRACTION

Figure 6 shows the measured process fluid sound speed and the gas void fraction determined using the measured process fluid sound speed, the liquid density, and the process pressure. The process pressure used in Wood's equation to interpret the gas void fraction was the measured pressure at the inlet of the Coriolis meter under test minus 70% of the difference of the pressure measured across the Coriolis meter.

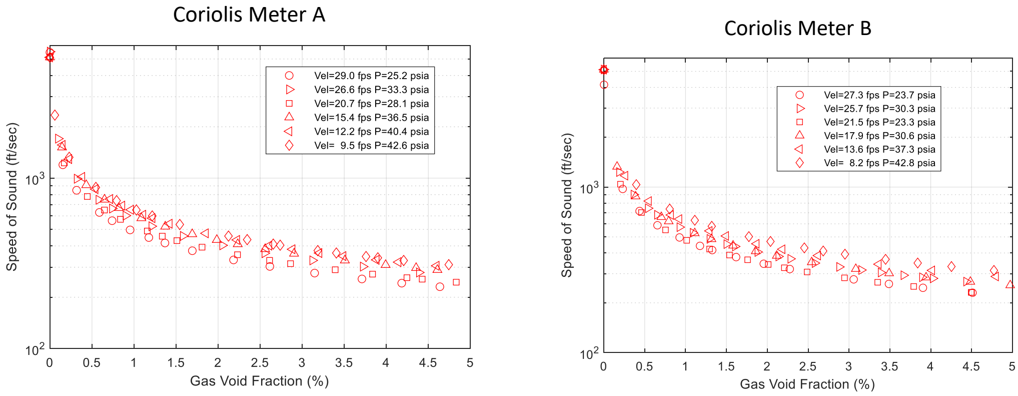

Figure 6: Measured Sound speed and interpreted Gas Void Fraction for a range of Mixture Velocities and Pressures

As shown, the measured process fluid speed of sound ranged from ~5000 ft/sec for liquid-only set points to ~200 ft/sec for the lower pressure points at 5% gas void fraction. The processing algorithms used in determining the process fluid sound speed from the array of pressure transducers determined the propagation speed and direction of the predominant sound propagating within the array. This measured propagation velocity was adjusted for the convection speed of the process fluid within the Coriolis meter under test to determine the thermodynamically-relevant speed of sound used in Wood's equation to determine the gas void fraction.

8 EXCITATION ENERGY METRICS DIAGNOSTICS

Each of the Coriolis meters tested had a diagnostic variable to indicate excitation energy input by the Coriolis meter to maintain the vibrational amplitude of the fluid-conveying flow tubes. This excitation energy diagnostic can provide important insight into the performance of Coriolis meters operating on bubbly flows [2]. For single-phase flows, the vibrating, fluid-conveying, flow tubes are typically lightly-damped. Under these conditions, the drive coil within the Coriolis meter is designed to have sufficient capability to maintain the vibration at a predetermined vibrational amplitude. However, with the introduction of entrained gases, relative motion between the gas bubbles and the fluid increases the effective damping within the fluid-conveying flow tubes. Modern Coriolis transmitter are designed to increase the excitation energy imparted into the vibrating flow tube to maintain a constant vibrational amplitude at the onset of, and increases in, gas void fraction. Although the quantitative relationship between gas void fraction and these respective excitation energy metrics can be quite complex, for bubbly flows, elevated levels of these excitation energy metrics are typically useful in the detection or entrained gases and correlate well with qualitative trends in gas void fraction levels.

Technical Paper

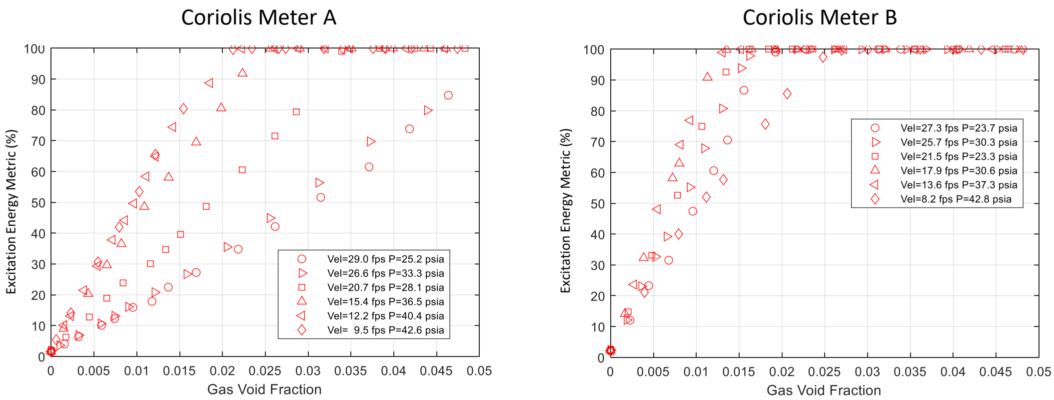

Figure 7: Excitation Energy Levels for Coriolis Meter A and Coriolis Meter B as a function of Gas Void Fraction for a Range of Mixture Velocities and Pressure

Figure 7 shows the excitation energy metric for Coriolis meter A and Coriolis meter B as a function of gas void fraction for a range of mixture velocities and pressures. Each excitation energy metric is plotted as a percentage of its maximum value. As shown, with the introduction of entrained gas, each Coriolis meter responds by increasing the excitation energy metric to maintain a predetermined vibrational amplitude. However, with additional increases in entrained gas levels, the excitation energy capability of each Coriolis meter eventually reaches its limit, at which point the excitation energy is said to be "saturated". Additional increases in entrained gas beyond this saturation condition result in reduced vibrational amplitude of the Coriolis meter. As shown, the gas void fraction at which the excitation energy saturated varies between the two meters and varies with operating conditions. As shown, a significant fraction of the data points presented in this paper was recorded from Coriolis meters operating with saturated excitation energy metrics.

In addition to an excitation energy metric, each of the meters tested provided a vibration amplitude metric. Figure 8 shows the flow tube vibrational amplitude for Coriolis meter A and Coriolis meter B as a function of gas void fraction for a range of mixture velocities and pressures. Note that the flow tube vibration amplitude diagnostic data from Coriolis meter A was recorded for flow rates, pressure, and gas void fractions that are similar, but not identical, to the data presented for Coriolis meter A throughout the rest of the paper. The amplitude of the vibration of Coriolis meter A and Coriolis meter B as a function of gas void fraction are related to the energy excitation metrics in qualitatively similar ways. As shown, for low gas void fraction conditions for which the excitation energy metric is not saturated, the amplitude of the tube vibration is 100%. However, once the excitation energy metric saturates, the amplitude of the tube vibration decreases with increasing gas void fraction, as expected [2]. For Coriolis meter A, the amplitude remained at 100% for the more fully-coupled flows for the full range of 0 to 5% gas void fraction. Whereas, for the more decoupled flows, the amplitude decreased to ~50% of the design amplitude at the highest gas void fraction (5%) presented. For Coriolis meter B, the amplitude decreased to 30% to 60% of the design amplitude at the highest gas void fraction (5%) presented, with the vibration amplitude not exhibiting a clear trend with mixture density-decoupling characteristics.

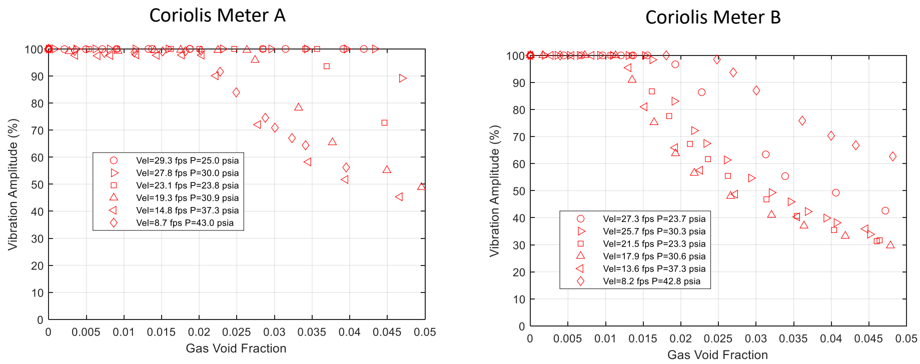

Figure 8: Flow Tube Vibrational Amplitude for Coriolis Meter A and Coriolis Meter B as a function of Gas Void Fraction for a Range of Mixture Velocities and Pressures

9 ROLE OF DECOULPING AND COMPRESSIBILITY

As developed above, aeroelastic models of Coriolis meters operating in bubbly flows predict that the errors due to decoupling scale with the gas void fraction, α, and errors due to compressibility scale with the square of the reduced frequency, f_{red}^2.

Figure 9 shows the square of the reduced frequency versus gas void fraction for the operating points tested for Coriolis meters A and B. Consistent with the approximate form of Wood's equation, the square of the reduced frequency scales essentially linearly with the gas void fraction. The increased square of the reduced frequency for a given gas void fraction of Coriolis meter B compared to Coriolis meter A indicates that compressibility effects are likely more important in Coriolis meter B than in Coriolis meter A.

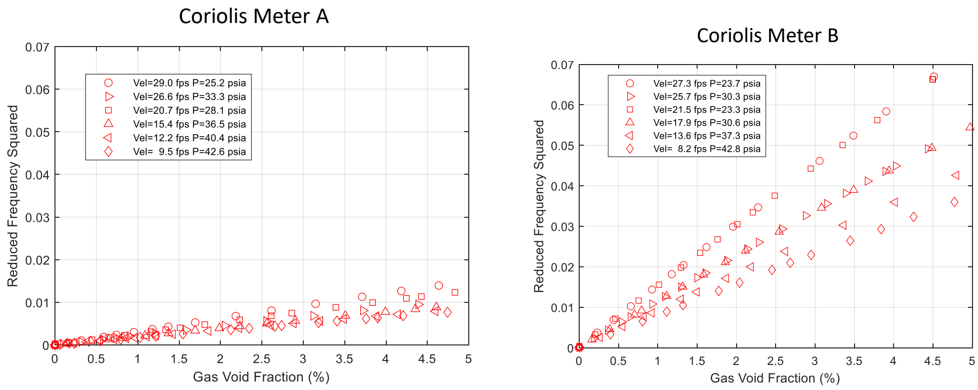

Figure 9: Square of the Reduced Frequency vs GVF to the Operating Points tested for Coriolis Meters A and B

10 DETERMINING DENSITY OF THE LIQUID PHASE

Augmenting Coriolis meters with a process fluid sound speed measurement provides a means to determine both the gas void fraction and the reduced frequency of a Coriolis meter. This information is useful in both characterizing the errors due to bubble flows, as well as compensating for these errors.

Determining the density of the liquid phase of a bubbly mixture is an important measurement for Coriolis meters for several reasons including 1) determining compositional information about the liquid, 2) for use as an input, along with the measured mass flow, to determine liquid volumetric flow rate, 3) and, as will be developed below, as an input for compensating for errors due to bubbly flows in the measured mass flow rate.

As developed above, for a bubbly mixture with essentially constant mixture properties but with varying gas void fraction, theoretical models predict that the effect of decoupling and compressibility combine such that the measured mixture density reported by a Coriolis meter that was calibrated for single-phase fluids trends linearly with gas void fraction, with the slope of this line representing the compressibility-adjusted density decoupling parameter, $K_{d_{eff}}$, defined above.

A least-squares optimization procedure was applied to the measured density versus gas void fraction data shown in Figure 4 for each data set with constant nominal flow rate and pressure, but varying gas void fraction, to determine optimized values for the liquid density and compressibility-adjusted density decoupling parameter for each data set. The results of this optimization for Coriolis Meter A are listed in Table 2 and the results for Coriolis meter B are listed in Table 3.

As shown the optimized compressibility-adjusted density decoupling parameter varied significantly as a function of mixture flow rates for each of the meters. The compressibility influence coefficient (Γ) is shown for each point well, indicating how the relative effects of compressibility will compare with effects of decoupling at a given gas void fraction will likely scale with the process pressure. The optimized liquid density for each of the data sets are also presented in Table 2 and Table 3 as well as the coefficient of determination (R2) for the linear fit of the measured density versus gas void fraction. As shown, the optimized liquid density for all data sets is quite close to unity. The coefficient of determination is also quite close to unity, indicating that the measured density versus gas void fraction data exhibits a high degree of linearity.

Table 2: Optimized Liquid Densities and Compressibility-adjusted Density Decoupling Parameters for Each Data set for Coriolis Meter A

Mixture Velocity (ft/sec)	Pressure (Psia)	Compressibility Influence Coefficient (Γ)	Compressibility-adjusted Density Decoupling Paramter (K_{deff})	Optimized Normalized Liquid Density	Coefficient of Determination (R^2)
29	25.2	0.19	0.87	1.0008	0.9953
26.6	33.3	0.14	0.85	1.0003	0.9982
20.7	28.1	0.17	1.10	1.0015	0.9957
15.4	36.5	0.13	1.44	1.0013	0.9955
12.2	40.4	0.12	1.74	1.0001	0.9984
9.5	42.6	0.11	2.10	0.9992	0.9991

Table 3: Optimized Liquid Densities and Compressibility-adjusted Density Decoupling Parameters for Each Data set for Coriolis Meter B

Mixture Velocity (ft/sec)	Pressure (Psia)	Compressibility Influence Coefficient (Γ)	Compressibility-adjusted Density Decoupling Paramter (K_{deff})	Optimized Normalized Liquid Density	Coefficient of Determination (R^2)
29.4	23.7	1.03	0.86	1.0008	0.9964
27.7	30.3	0.81	1.21	1.0022	0.9908
23.2	23.3	1.05	1.45	1.0029	0.9928
19.3	30.6	0.80	1.93	1.0031	0.9958
14.6	37.3	0.65	2.44	1.0021	0.9991
8.8	42.8	0.57	3.00	1.0006	0.9953

Figure 10 shows measured density (open symbols) and the corrected liquid density (green filled symbols) for Coriolis meters A and B operating over a range of bubbly flows. The corrected liquid density shown in Figure 10 was determined utilizing the measured density and measured gas void fraction at each point and applying the compressibility-adjusted density decoupling parameter identified for each data set and listed in Table 2 and Table 3 as follows:

$$\rho_{liq} \cong \frac{\rho_{measured}}{\left(1 - K_{deff}\,\alpha\right)} \qquad (18)$$

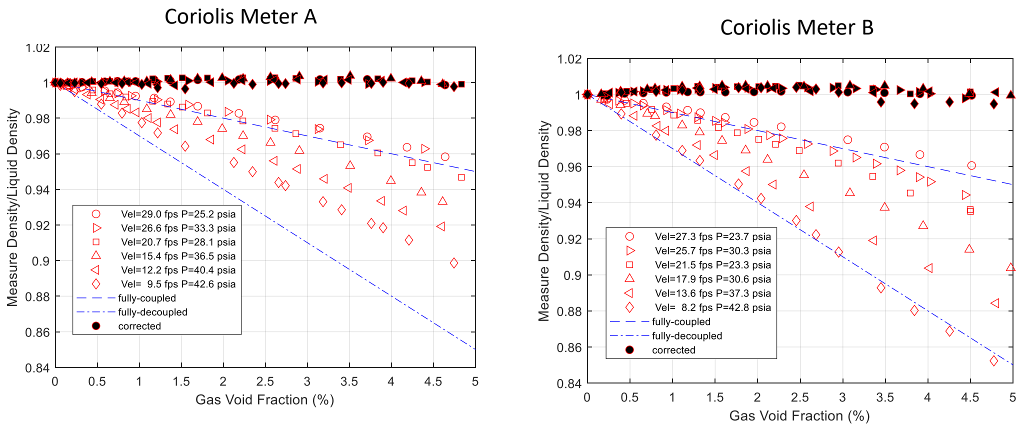

Figure 10: Measured Density and Corrected Liquid Density for Coriolis Meter A and Coriolis Meter B operating in Bubbly Flows

Although Coriolis meters subject to entrained gases in the field are unlikely to be exposed to as wide a range of gas void fraction (0 to 5%) over a period of time in which the liquid density, mass flow rate, and pressure are maintained at constant levels, the linearity of measured density data versus gas void fraction can be exploited in a variety of ways to effectively determine the density of the liquid phase of bubbly mixture with variable gas void fraction using a speed of sound augmented Coriolis meter. For example, Gysling and Dragnea [13] presented experimental data on a speed of sound augmented Coriolis meter providing a density-based watercut on the liquid outlet of a compact gas-liquid separator in the presence of variable amounts of gas carry-under. This work demonstrated the ability of speed of sound augmented Coriolis meters to effectively measure the liquid density of bubbly mixtures of oil, water, and gas with varying gas void fraction. The measured liquid phase density was used to provide accurate density-based water cut measurement, in the presence of variable amounts of gas carry-under, utilizing a Coriolis meter on bubbly oil-water-gas mixtures exhibiting a wide range of decoupling characteristics.

11 CORRELATING MASS FLOW AND DENSITY ERRORS

The approach developed herein to compensate for mass flow errors due to bubbly flow is based on defining and correlating a mass flow error parameter with a density error parameter for bubbly flows. The approach is motivated by first-principles aeroelastic models of the errors developed in Coriolis meters operating in bubbly flows which predict that the errors in mass flow and density have similar dependencies on the decoupling and compressibility mechanisms. In this approach, a non-dimensional mass flow error parameter, Φ, is defined as a parametric function of measured mass flow rate, liquid mass flow rate, gas void fraction, and reduced frequency.

Similarly, a non-dimensional density error parameter, Ψ, is defined as a parametric function of measured density, liquid density, gas void fraction, and reduced frequency. Using a reference data set for a Coriolis meter operating over a range of bubbly flow conditions, such as the data sets presented for Coriolis meter A and B above, weighting parameters in the non-dimensional mass flow error parameter, Φ, and the non-dimensional density error parameter, Ψ, are optimized to maximize the correlation between the mass flow error parameter and the density error parameter over the data set. This methodology of augmenting an existing Coriolis meter with a process fluid sound speed measurement is shown schematically in Figure 11. As indicated, the functionality of the existing Coriolis meter is unaltered, with the mass flow and density reported by the existing Coriolis meter providing the basis of the speed-of-sound corrected values.

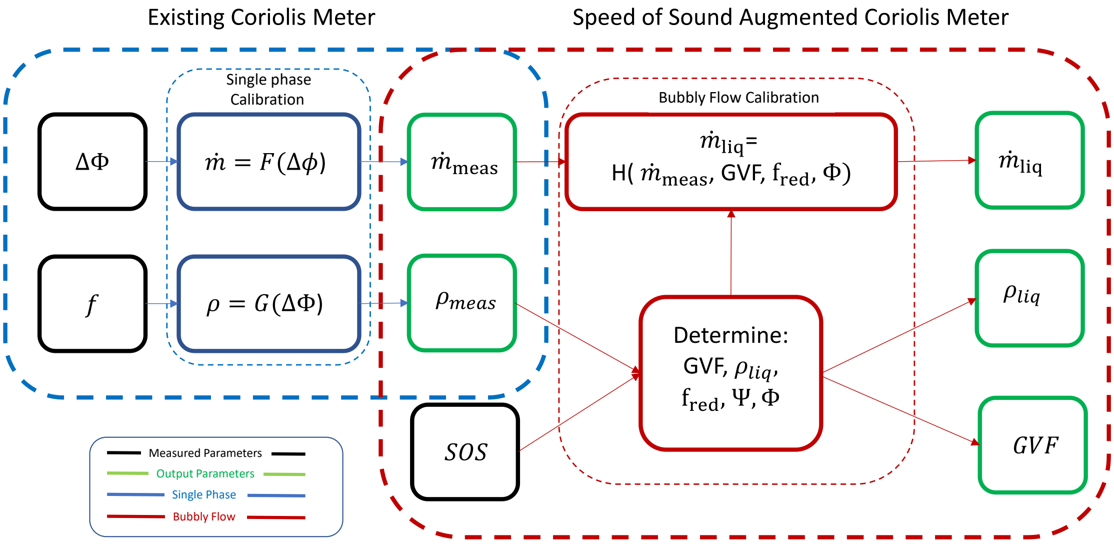

Figure 11: Schematic of Method used to augment the output of a Coriolis Meter with a Process Fluid Speed of Sound Measurement

Figure 12 shows optimized non-dimensional mass flow error parameters plotted versus non-dimensional density error parameters for the data sets presented for Coriolis meter A and Coriolis meter B, as well as a curve-fit of the data. As shown, the mass flow error parameters and the density error parameters are highly correlated over range of data presented.

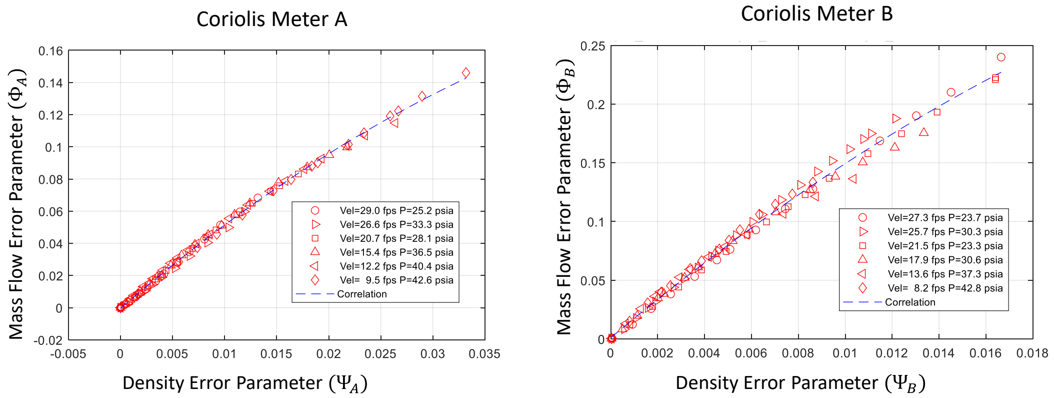

Figure 12: Non-Dimensional Mass Flow Error Parameter vs Non-Dimensional Density Error Parameters Optimized for the Data Sets Presented for Coriolis Meters A and B

Optimized weighting parameters for a given Coriolis meter will, in general, depend on the design parameters of the Coriolis meter as well as the range of decoupling characteristics and compressibility influence coefficients within the reference data sets. For example, for the pressures and conditions tested, the compressibility influence parameter for Coriolis meter A is significantly smaller than unity for the entire data set ($0.11<\Gamma<0.19$), indicated that decoupling effects, compared to compressibility effects, are likely the predominant source of errors due to bubbly flows. Whereas, for Coriolis meter B, the compressibility influence coefficient is closer to unity ($0.57<\Gamma<1.05$), indicating that errors due to compressibility will likely play a more comparable role to errors associated with decoupling for Coriolis meter B at the pressures tested. Since the two meters were tested over similar operating conditions, difference in the compressibility influence parameters is primarily due to the difference in the vibration frequencies of the two meters. If, however, for example, similar tests were conducted at significantly higher pressures, the compressibility influence coefficients would be reduced for each of the meters. This would likely have a limited effect on Coriolis meter A, for which the compressibility influence coefficients for this data set are currently small compared to unity. However, this increase in pressure would likely have a more significant effect on the Coriolis Meter B for which the compressibility influence coefficient would be reduced from near unity to significantly less than unity.

12 CORRECTING MASS FLOW ERRORS

For bubbly mixtures for which the liquid density is known, or determined, the density error parameter is readily determined at each operating condition using the liquid density, the measured density and speed of sound, and density error weighting parameters. The mass flow error parameter can then be determined utilizing a design-specific correlation between the mass flow error parameter and the density error parameter, such as those shown in Figure 12. The measured mass flow rate can then be compensated based on the determined mass flow error parameter, the gas void fraction, the reduced frequency, and mass flow error weighting parameters.

The process described above was applied to the mass flow and density errors measured for Coriolis meter A and B operating in bubbly flow flows. Figure 13 shows the measured (open symbols) and compensated mass flow rates (filled symbols) determined utilizing the correlations developed relating the mass flow error parameter to the density error parameter for each meter.

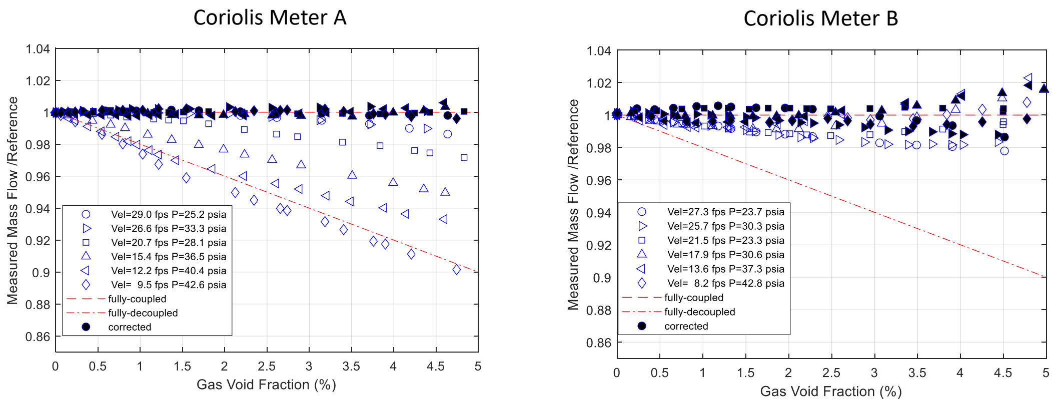

Figure 13: Measured and Corrected Mass Flow for Coriolis Meter A and B operating in Bubbly Mixtures over a range of Mixture flow Velocities and Pressures

As shown, the errors in the measured mass flow are significantly reduced for Coriolis meter A, and, to lesser extent, improved for Coriolis B as well.

13 CORRECTING LIQUID VOLUMETRIC FLOW ERRORS

The corrected liquid density and the corrected mass flow can then be used to determine a corrected liquid volumetric flow. Figure 14 shows the volumetric flow rate determined from the measured mass flow rate and measured density (open symbols) and the corrected liquid volumetric flow rate (filled symbols), determined using the corrected mass flow rate and the corrected liquid density.

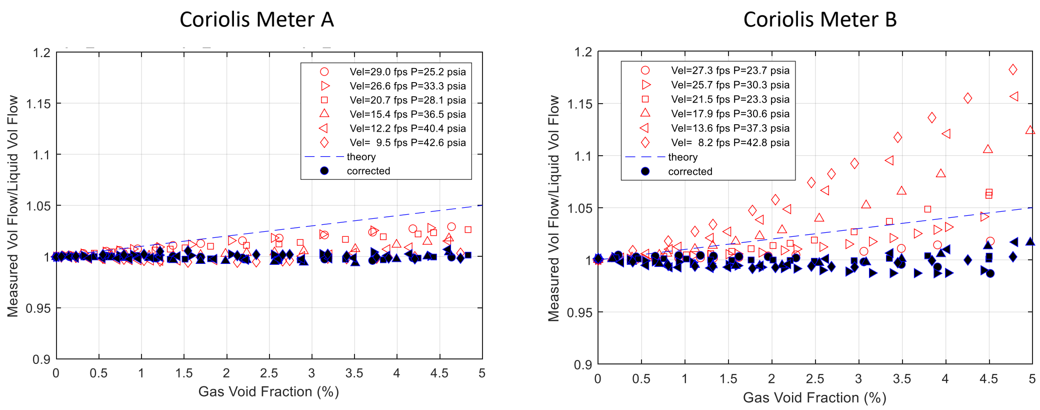

Figure 14: Measured and Corrected Liquid Volumetric Flow For Coriolis Meter A and Coriolis Meter B operating in a Bubbly Flow

As shown, errors in the liquid volumetric flow rates for the bubble flows are significantly reduced using corrected mass flow and corrected liquid densities.

14 DISCUSSION AND CONCLUSIONS

Data presented herein demonstrate that augmenting the output of Coriolis meters with a process fluid speed of sound measurement can significantly improve the accuracy of Coriolis-based flow measurement of bubbly flows. By utilizing an array of pressure transducers installed external to the Coriolis meter under test to measure the process fluid speed of sound, the methodology presented herein does not impact the operation the Coriolis meter under test. Instead, the methodology utilizes the mass flow and density reported by the Coriolis meter operating in bubbly flows as the input to a compensation methodology in which the output of the Coriolis meter and a process fluid speed of sound measurement are used within an empirically-informed, first-principles aeroelastic models to provide corrected mass flow, density, volumetric flow and gas void fraction of bubbly flows. As such, this approach can be implemented on a minimally-intrusive basis on existing Coriolis meters operating on either known, or suspected, bubbly flow conditions without impacting the current operation of the Coriolis meter. In this way, the new information provided by measuring the process fluid sound speed and correcting the mass flow, density, volumetric flow, and gas void fraction can be evaluated along with the existing output from the existing Coriolis meter.

The data presented on the mass flow and density errors associated with bubbly flows are broadly consistent with theoretical models of errors in Coriolis meters operating on bubbly flows. Consistent with theory, the data indicate that Coriolis meters begin to report errors due to bubbly flow with the onset of gas void fraction, and the errors in both mass flow and density generally increase with increasing gas void fraction. Furthermore, the errors on mass flow and density were shown to scale with gas void fraction.

For the conditions tested, the compressibility influence coefficients, Γ, indicate that, theoretically, the errors observed Coriolis meter A ($\Gamma \ll 1$) were likely predominantly due to decoupling effects, and that errors observed in Coriolis meter B ($\Gamma \sim 1$) were likely due to a more balanced mix of compressibility and decoupling effects.

Bubbly flows within the vibrating flow tubes of Coriolis meters are inherently complex flows, the detailed characteristics of which, such as fluid viscosity, surface tension, gas void fraction, bubble size and distribution, are often unknown and time-varying; thereby making a-prior predictions for the effects of bubbly flows on Coriolis meters quite difficult. Although the data presented herein was limited to water and air mixtures at relatively low pressures, the results indicate that conditions tested in this work spanned a wide range of the key non-dimensional parameters that influence errors associated with Coriolis meters operating on bubbly flows including 1) gas void fraction, 2) compressibility-adjusted density decoupling parameter, $K_{d_{eff}}$,and 3), the compressibility influence coefficients, Γ. Thus, although additional testing on a wider range of fluids, operating conditions, and Coriolis meter model numbers is planned, the results presented herein and in other work [13] suggest that the methods described herein are applicable to a wide range of bubbly flow applications.

Additionally, the data indicate that Coriolis meters can exhibit a wide range of errors associated with decoupling on a given gas / liquid mixture, and the amount of decoupling for a given gas/liquid mixture can vary significantly over a limited range of mixture flow velocities. Quantitatively, the errors due to bubbly flows in mass flow and density for a given meter can be distinct, and the errors due to bubbly flows in mass flow, density, and volumetric flow for different Coriolis meters can have distinctly different characteristics.

Diagnostic data on the excitation energy metrics and flow tube vibrational amplitude indicate that, for bubbly flows with varying gas void fraction, but all other relevant parameters held essentially constant, excitation energy metrics increase with gas void fraction. The vibration amplitude remains constant as the excitation energy metric increases, until the excitation energy metric saturates. Once saturated, the excitation energy metric remains constant, and additional increases in gas void fraction result in reduced flow tube vibration amplitude. Data presented indicates that the two modern Coriolis meters tested can continue to provide correctable measured mass flow and density measurements for operating conditions beyond conditions at which the energy excitation metrics are saturated, and for which the amplitude of vibration decreases significantly below the design vibrational amplitude. Quantifying the impact of this reduction in flow tube vibrational amplitude on the mass flow and density measured by the Coriolis meter is beyond the scope of this work, but it seems reasonable to postulate that there would be a minimum vibrational amplitude required for Coriolis meters to report correctable mass flow and/or density using the methods described herein.

14 NOTATION

α	gas void fraction
δ	inverse Stokes parameter
ρ	density
φ	volumetric phase fraction
μ	dynamic viscosity
Ψ	density error function
Φ	mass flow error function
Γ	compressibility influence parameter
a	speed of sound
D	diameter
f	frequency
F	mass flow calibration function
G	density calibration function
K_d, K_m	decoupling parameter
G_d, G_m	compressibility parameter
$\dot{m}$	mass flow rate
R	radius
Q	volumetric flow rate

15 REFERENCES

[1] Wang T. and Baker, R., "Coriolis Flow Meters: A review of the developments over the past 20 years, and an assessment of the state of the art and likely future directions", Journal of Flow Measurement and Instrumentation 40 (2014) pp99-123

[2] Weinstein, Joel, "Multiphase Flow in Coriolis Mass Flow Meters – Error Sources and Best Practices", 28th International North Sea Flow Measurement Workshop 26th – 29th October 2010.

[3] Henry, M., Clarke, D.,Vignos, J., "Coriolis Flowmeter with Digital Control System", European Patent EP0919793

[4] Cage, D., Dragnea, G., "System and Method for Fluid Compressibility Compensation in a Coriolis Mass Flow Meter", US Patent 6502466, 2003

[5] Hemp, J., and Kutin, J. "Theory of errors in Coriolis flowmeter readings due to compressibility of the fluid being metered", Journal of Flow Measurement and Instrumentation, Volume 17, Issue 6, December 2006, Pages 359-369

[6] Gysling, D, "An Aeroelastic model of Coriolis mass and density meters operating on aerated mixtures" Journal of Flow Measurement and Instrumentation, Volume 18, Issue 2, April 2007, Pages 69-77

[7] Weinstein, Joel, "The Motion of Bubbles and Particles in Oscillating Liquids with Applications to Multiphase Flow in Coriolis Meters", PhD Thesis, Department of Mechanical Engineering, University of Colorado, 2008

[8] Zhu, Hao, Application of Coriolis Mass Flowmeters in Bubbly or Particulate Two-Phase Flows, PhD. Thesis, Institute of Fluid Mechanics, University of Erlangen-Nuremberg, Shaker Verlag, 2009

[9] Ward, Eric, "New Class of Flow Meter Solves Old Problem Impacting Well Test Accuracy", SPE Paper 100893, Western Regional Joint Meeting, Anchorage, Alaska, 2006

[10] Gysling, D. et al, "Apparatus and Method for Compensating a Coriolis Meter", US Patent 7,152.460, December 2006

[11] Temkin, S., "Sound Propagation in Bubbly Liquids" Naval Research Laboratory Memorandum Report 6403, 5 April 1989

[12] Evans, G. Jameson, G. Atkinson, B. "Prediction of Bubble Size Generated by a Plunging Liquid Jet Bubble Column", Chemical Engineering Science, Vol 47, No. 13/14, pp.3265-3272, 1992

[13] Gysling, D., Dragnea, G., "Density-based Watercut using a Speed-of-Sound Augmented Coriolis Meter on a Gas/Liquid Separator with Variable Gas Carry-Under", 38th International North Sea Flow Measurement Workshop 26-29 October 2020